Dalton Transactions

PAPER

View Article Online
View Journal | View Issue

Cite this: *Dalton Trans.*, 2014, **43**, 706

A highly fluorescent chemosensor for Zn^{2+} and the recognition research on distinguishing Zn^{2+} from Cd^{2+}†

Pengxuan Li,[a] Xiaoyan Zhou,[a] Ruoying Huang,[b] Lizi Yang,[a] Xiaoliang Tang,[a] Wei Dou,[a] Qianqian Zhao[a] and Weisheng Liu*[a]

Received 8th August 2013,
Accepted 25th September 2013

DOI: 10.1039/c3dt52165f

www.rsc.org/dalton

A new fluorescent sensor, 2-(2-oxo-2-(quinolin-8-ylamino)ethoxy)-*N*-(pyridine-2-ylmethyl) benzamide (L), composed of a quinoline group as the fluorogenic unit and a pyridin-2-ylmethanamine as the binding unit for metal ions has been synthesized. The sensor shows excellent selectivity and sensitivity with a fluorescence enhancement to Zn^{2+} over other cations in acetonitrile aqueous solution. The X-ray crystal structure analysis reveals that sensor L coordinates to Zn^{2+} *via* a 1 : 1 binding mode but to Cd^{2+} *via* a 2 : 1 binding mode, which lead to a different spatial arrangement of the fluorogenic unit in these complexes. In addition, density functional theory calculations on L, and the Zn^{2+}/L and Cd^{2+}/L complexes also imply that the different structures of L significantly affect the molecular orbital energy levels and electron transition, which would result in the spectral changes to distinguish Zn^{2+} from Cd^{2+}. The absorption study results may also suggest the Cd^{2+} in the complex can be displaced by Zn^{2+}. Furthermore, the fluorescence imaging of Zn^{2+} in living cells was obtained.

Introduction

Fluorescent chemosensors have been developed to be useful tools to sense *in vitro* and *in vivo* biologically important species such as metal ions and anions because of the simplicity and high sensitivity of fluorescence assays.[1] As the second-most abundant transition metal following iron in the human body, Zn^{2+} plays diverse roles in biological processes such as brain function, gene transcription, immune function, mammalian reproduction and others.[2] For example, over 90% of the Zn^{2+} found in the brain and the body is classified as static, playing structural roles in transcription factors and related proteins as well as structural and catalytic roles in enzymes.[3] In addition, many pathological processes such as epilepsy, ischemic stroke, Alzheimer's disease (AD), amyotrophic lateral sclerosis (ALS), Guam ALS-Parkinsonism-dementia Parkinson's disease and infantile diarrhea involve intracellular zinc ions.[4] The growing contributions of zinc homeostasis in sustaining life have prompted an interest in devising new ways to detect Zn^{2+} in biological samples.[5] Up to now, fluorescence detection stands out as the most effective means to monitor Zn^{2+} in biological systems because it is spectroscopically or magnetically silent due to its d^{10} electron configuration.[6]

In fact, much effort has been made to develop fluorescent chemosensors to detect Zn^{2+} in the past few years. However, it is still a challenge to explain the reason for the selective fluorescent change of the chemosensors to distinguish Zn^{2+} from Ca^{2+}, Mg^{2+} or Cd^{2+}, because the chelators for Zn^{2+} usually show a certain degree of affinity for others. In particular, Cd^{2+} is in the same group of the periodic table and has similar properties to Zn^{2+}, which usually causes similar spectral changes after coordinating with fluorescent sensors.[7] Therefore there is a great requirement for developing and researching the recognition mechanism of Zn^{2+}-selective sensors which can discriminate Zn^{2+} from Cd^{2+} with a high sensitivity and selectivity.

Quinoline and its derivatives, particularly 8-hydroxyquinoline and 8-aminoquinoline, are well-known fluorogenic agents and potential binding units for quantitative chemical assays of some metal ions, especially Zn^{2+}.[8] We have previously reported some sensors that can exhibit a Zn^{2+}-specific fluorescent response.[7b,9] To improve the water solubility and selectivity toward Zn^{2+}, we present a simple 8-aminoquinoline-based fluorescence chemosensor L, combined with a salicylic spacer with an appended quinoline group and a pyridin-2-ylmethanamine group for binding metal ions. Upon binding Zn^{2+}, L shows excellent selectivity and sensitivity with a fluorescence enhancement to Zn^{2+} over other cations in acetonitrile aqueous solution. The bright "switch-on" state is based on the efficient inhibition for the PET process in HEPES buffer, accompanied by increasing the coplanarity of the ligand and

[a]*Key Laboratory of Nonferrous Metals Chemistry and Resources Utilization of Gansu Province, State Key Laboratory of Applied Organic Chemistry, College of Chemistry and Chemical Engineering, Lanzhou University, Lanzhou 730000, China. E-mail: liuws@lzu.edu.cn; Fax: +86-931-8912582; Tel: +86-931-8915151*
[b]*West China School of Public Health, Sichuan University, Chengdu 610041, China*
†Electronic supplementary information (ESI) available. CCDC numbers 942962 and 942963. For ESI and crystallographic data in CIF or other electronic format see DOI: 10.1039/c3dt52165f

reducing the loss of energy *via* non-radiative transitions. But Cd^{2+} could cause L a distinct emission, which afforded the neutral complex $CdL_2(NO_3)_2$ characterized by single-crystal X-ray structural determination. The difference in radius between Cd^{2+} (0.96 Å) and Zn^{2+} (0.74 Å) could be responsible for the alteration in the coordination structure and the extent of the CHEF effect on the chromophores. Meanwhile, the spin–orbit quenching mechanism associated with heavy metals and the weaker Lewis acidity of Cd^{2+} in comparison with Zn^{2+} may also account for the difference in the fluorescence intensity.[10] Additionally, the recognition mechanisms of L toward Zn^{2+} and Cd^{2+} were further attempted to explain by computational results. The sensing properties of L toward Zn^{2+} over other biologically relevant metal ions were investigated in detail, and the fluorescence imaging of Zn^{2+} in living cells was also conducted to establish the capability in a practical application.

Experimental section

Material and methods

All chemicals for the synthesis were purchased from commercial sources and used without further purification. All of the solvents were of analytical reagent grade. The HEPES buffer solutions (50 mM, 30 mM NaCl, pH = 7.40) were prepared in CH_3CN–H_2O (1 : 1, v/v). All pH measurements were made with a pH-10C digital pH meter. ^1H NMR (400 MHz) and ^{13}C NMR (100 MHz) spectra were taken on a BrukerDRX400 spectrometer in a $CDCl_3$ solution with TMS as the internal standard. The ESI-TOF mass spectrum was recorded on Mariner MS spectrometer. The FT-IR spectra were recorded on a Nicolet FT-170SX instrument using KBr discs in the 400–4000 cm^{-1} region. The melting point was measured on a Kofler apparatus. The absorption spectra were performed on a Varian Cary 100 spectrophotometer equipped with quartz cells of 1.0 cm path length. The fluorescence spectra were obtained using the Edinburgh Instrument FLS920 using quartz cuvettes of 1.0 cm path length with a xenon lamp as the excitation source. The absolute quantum yields were determined using an Edinburgh Instrument FLSP920. All of the measurements were conducted at room temperature unless otherwise stated.

Synthesis of L

The preparation of 2-(2-oxo-2-(quinolin-8-ylamino)ethoxy)-*N*-(pyridine-2-ylmethyl)benzamide (L). Anhydrous potassium carbonate (897 mg, 6.5 mmol) was added to a solution of 2-hydroxy-*N*-(pyridine-2-ylmethyl)benzamide (1.14 g, 5 mmol)[11] in *N*,*N*-dimethylformamide (30 mL), and the mixture was stirred and held at reflux. 2-Chloro-*N*-(quinol-8-yl)-acetamide (1.1 g, 5 mmol)[9b] in 5 mL *N*,*N*-dimethylformamide was added dropwise to the mixture an hour later. After further stirring at reflux for another 24 hour, the mixture was cooled to room temperature and removed by vacuum filtering. The filtrate was successively extracted with dichloromethane, saturated salt water and then dried with Na_2SO_4. The solvents were evaporated to obtain a crude product, which was purified by a silica gel column chromatography using petroleum–ethyl acetate (10 : 1, v/v). Yield: 70% (1.28 g). Mp: 160.8–161.7 °C. Anal. calcd for $C_{24}H_{20}N_4O_3$: C, 68.87; H, 4.377; N, 13.30. Found: C, 69.89; H, 4.89; N, 13.58. FT-IR (KBr pellet, cm^{-1}): 3431 (br), 3254 (m), 1673 (m), 1648 (s), 1598 (m), 1540 (vs), 1487 (m), 1429 (m), 1325 (m), 1295 (w), 1248 (m), 1164 (w), 756 (m) (br, broad; w, weak; m, medium; s, strong; vs, very strong); ^1H NMR (400 Hz, $CDCl_3$, ppm): δ 10.65(–NHCO, s, 1H), 8.96 (Q-NHCO, s, 1H), 8.72(dd, 1H), 8.68(dd, 1H), 8.23(m, 2H), 8.08 (dd, 1H), 7.50(m, 3H), 7.38(dd, 1H), 7.31(td, 1H), 7.18(t, 1H), 7.08(d, 1H), 7.03(d, 1H), 6.81(dd, 1H), 4.97(–$COCH_2$, s, 2H), 4.80(–CONH–CH_2, dd, 2H). ^{13}C NMR (100 Hz, $CDCl_3$, ppm): δ 165.65, 165.20, 156.13, 155.24, 148.48, 148.35, 138.26, 136.03, 135.93, 133.27, 132.72, 132.26, 127.67, 126.95, 123.31, 122.63, 122.19, 121.65, 121.53, 121.21, 116.64, 112.77, 68.69, 45.07. ESI-MS: *m*/*z* 413.3 [$(M + 1)^+$]. HRMS (ESI): *m*/*z* calcd for $C_{24}H_{20}N_4O_3 + H^+$: 413.1604; found 413.1608. (Scheme 1).

Synthesis of $ZnL(NO_3)_2(H_2O)$. A 10 mL acetonitrile solution of $Zn(NO_3)_2{\cdot}6H_2O$ (0.0149 g, 0.05 mmol) was added to a stirred 5 mL methanol solution of the ligand L (0.0206 g, 0.05 mmol). The reaction mixture was stirred in air for 4 h and filtered. The filtrate was kept in air. After evaporation for 4 days, yellow block single crystals of $ZnL(NO_3)_2(H_2O)$ suitable for X-ray crystallography were obtained. Anal. calcd for $C_{24}H_{22}N_6O_{10}Zn$: C, 46.045; H, 3.7025; N, 12.875. Found: C, 46.50; H, 3.58; N, 13.56. FT-IR (KBr pellet, cm^{-1}): 3473 (br), 3263 (m), 1706 (m), 1611 (s), 1547 (vs), 1477 (vs), 1462 (vs), 1384 (m), 1308 (m), 1282 (s), 1025 (m), 814 (m), 615 (m).

Synthesis of $CdL_2(NO_3)_2$. This complex was prepared by the same synthetic procedure as that of $ZnL(NO_3)_2(H_2O)$ and colorless block single crystals of $CdL_2(NO_3)_2$ were obtained after evaporation for a week. Anal. calcd for $C_{48}H_{40}N_{10}O_{12}Cd$: C, 53.14; H, 3.946; N, 13.14. Found: C, 54.32; H, 3.80; N, 13.20. FT-IR (KBr pellet, cm^{-1}): 3349(m), 3301(m), 1687(s), 1612(vs),

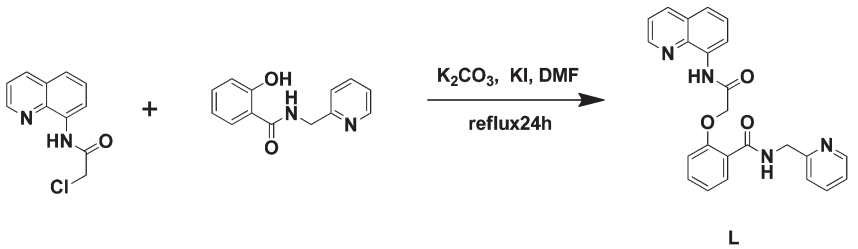

Scheme 1 Synthesis of L.

1576(m), 1552(vs), 1488(s), 1440(s), 1422(s), 1297(s), 1241(m), 1232(m), 1159(m), 1029(m), 751(m), 613(m).

X-ray diffraction studies

Single-crystal X-ray diffraction measurements were performed on a Bruker SMART 1000 CCD diffractometer operating at 50 kV and 30 mA using Mo Kα radiation (λ = 0.71073 Å). The crystal was mounted inside a Lindemann glass capillary for data collection using SMART and SAINT software.[12] An empirical absorption correction was applied using the SADABS program.[13] The structure was solved by direct methods and refined by full-matrix least squares on F^2 using the SHELXTL-97 program package.[14] The crystallographic data and details of the structure for $ZnL(NO_3)_2(H_2O)$ and $CdL_2(NO_3)_2$ are summarized in Tables S1 and S2 in the ESI.† CCDC numbers 942962 and 942963 contain the supplementary crystallographic data for this paper.

Theoretical calculations

Theoretical investigations on L, L–Cd^{2+} and L–Zn^{2+} by the GAUSSIAN 09 program suite[15] were performed at the B3LYP level and the LANL2DZ effective core potential was used for all of the atoms.[16] The optimized structures of the complexes were very close to their single crystal X-ray diffraction structures.

Results and discussion

Absorption study

To obtain an insight into the binding mechanism of L toward metal ions, the UV-Vis spectra of L in an acetonitrile solution was investigated and is shown in Fig. 1. The absorbance of L at 316 nm gradually decreases and a new absorption appears at 363 nm with the addition of Zn^{2+}. The isosbestic point at 336 nm might be attributable to the coordination between L and Zn^{2+}. The absorbance at 316 and 363 nm shows a linear change until the ratio of $[Zn^{2+}]:[L]$ reaches 1 : 1, and no longer changes with continuously titrated of Zn^{2+}. It is suggested that the stoichiometry between L and Zn^{2+} is 1 : 1, which is consistent with the results of the Job's plot and the crystal structure. On the other hand, the absorbance of L at 295 nm slightly increased depending on the concentration of Cd^{2+}, and was almost saturated after the addition of 0.5 equiv. Cd^{2+} (Fig. S5†). Furthermore, the introduction of Zn^{2+} to the L–Cd^{2+} complex caused a new absorption at 363 nm (Fig. S6†). The results may imply that the Cd^{2+} in the complex can be displaced by Zn^{2+}. To evaluate whether this property can be preserved in a CH_3CN–H_2O mixed solvent, we also carried out the absorbance titration in HEPES buffer (50 mM, 30 mM NaCl, pH = 7.40, CH_3CN–H_2O = 1 : 1, v/v) as shown in Fig. S1.†

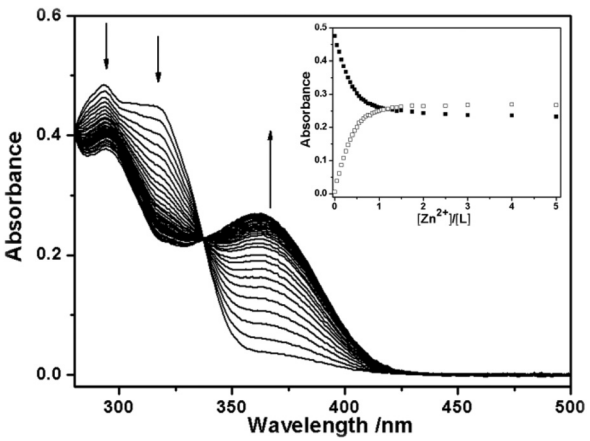

Fig. 1 The absorption spectra of L in acetonitrile with the increase of $Zn(NO_3)_2$. Inset: the absorbance at 363 nm (□) and 316 nm (■) varied as a function of $[Zn^{2+}]:[L]$. $[L] = 1.0 \times 10^{-4}$ M.

Fluorescence spectra and titration

L exhibited a weak fluorescence with quantum yield (Φ = 0.0675) in acetonitrile, which was much lower than that (Φ = 0.333) in the presence of Zn^{2+}. The titration of Zn^{2+} in the solution of L resulted in a remarkable increase of emission at 498 nm and a more than 75-fold fluorescence enhancement was observed (Fig. S7†). The fluorescence intensity was almost proportional to the Zn^{2+} concentration when the ratio of $[Zn^{2+}]:[L]$ was less than 1, supporting the 1 : 1 stoichiometry as well.

When considering the practical application of the fluorescent probe in aqueous solution, the fluorescence sensing ability of L was examined in HEPES buffer (50 mM, 30 mM NaCl, pH = 7.40, CH_3CN–H_2O = 1 : 1, v/v). The addition of water to the solvent led to the fluorescence quenching of the complexes and L to a certain degree, but the fluorescence change was also obvious when Zn^{2+} was introduced. The fluorescence intensity increased up to 46-fold in the presence of 5 equiv. Zn^{2+} (Fig. 2). The nonlinear-fitting analysis of the change in the fluorescence intensity illustrated the binding

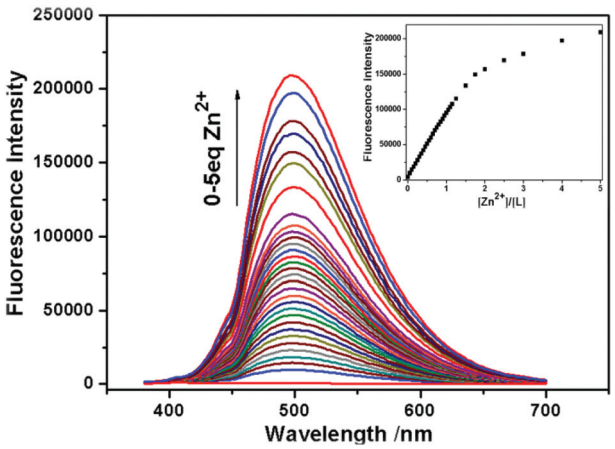

Fig. 2 The fluorescence emission spectra of L upon the addition of $Zn(NO_3)_2$ in HEPES buffer (50 mM, 30 mM NaCl, pH = 7.4, CH_3CN–H_2O = 1 : 1, v/v). λ = 363 nm at room temperature ([L] = 0.10 mM.) (Inset) The corresponding $Zn(NO_3)_2$ titration profile according to the fluorescence intensity, indicating a 1 : 1 stoichiometry for Zn^{2+} : L.

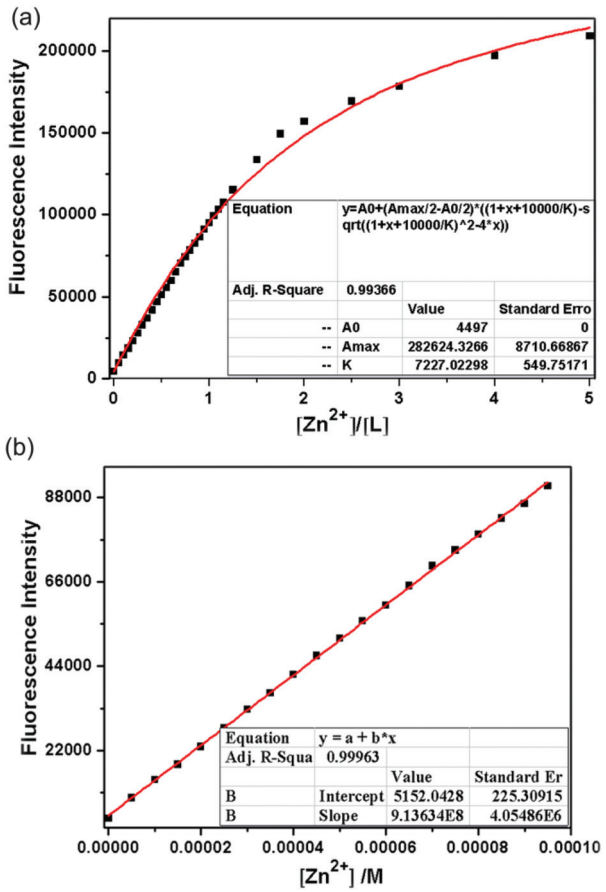

Fig. 3 (a) A change in the fluorescence intensity at 498 nm. The red line is the nonlinear fitting curve obtained assuming a 1 : 1 association between L and Zn^{2+}. λ_{max}ex = 363 nm, [L] = 0.1 mM. (b) The linear dynamic response of L for Zn^{2+} and the determination of the detection limit (LOD) for Zn^{2+} in HEPES buffer (50 mM, 30 mM NaCl, pH = 7.4, $CH_3CN–H_2O$ = 1 : 1, v/v). The LOD was calculated by multiplying the standard derivation of 13 blank measurements by three and dividing by the slope of the linear calibration curve at a lower concentration.

constant of 7.3×10^3 M^{-1} for Zn^{2+} in aqueous solution (R^2 = 0.9937, Fig. 3a). The detection limit (LOD) was measured to be 4.9×10^{-8} M (3σ per slope) (R^2 = 0.9996, Fig. 3b).

The selectivity of L was also evaluated in the HEPES buffer (Fig. 4). The introduction of Na^+, K^+, Li^+, Mg^{2+}, Ca^{2+}, Mn^{2+}, Hg^{2+}, Co^{2+}, Pb^{2+}, Ni^{2+}, Cu^{2+}, Al^{3+}, Cr^{3+} and Fe^{3+} quenched the emission to some extent. This phenomenon may be due to the non-radiative energy transition in the process of electron or energy transfer between the d orbital of the ions and the fluorophore.[17] However, the addition of Cd^{2+} induced almost no changes in the emission. These results indicated that L can serve as a selective fluorescent chemosensor for Zn^{2+} in aqueous solutions as well.

Metal ion competition studies

The response of L to Zn^{2+} in the presence of other competing ions was demonstrated in HEPES buffer (50 mM, 30 mM NaCl, pH = 7.40, $CH_3CN–H_2O$ = 1 : 1, v/v) to further assess the selectivity of L for Zn^{2+} (Fig. 5). The fluorescence intensity of the

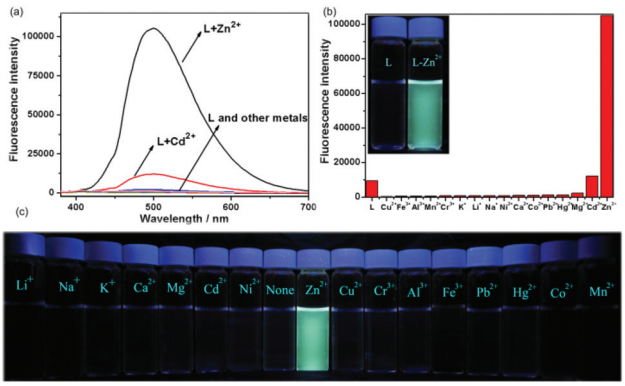

Fig. 4 (a) The fluorescence spectra of probe L in the absence and presence of different metal ions Li^+, Na^+, K^+, Ca^{2+}, Mg^{2+}, Cr^{3+}, Mn^{2+}, Fe^{3+}, Co^{2+}, Ni^{2+}, Cu^{2+}, Zn^{2+}, Cd^{2+}, Al^{3+}, Pb^{2+} and Hg^{2+} (as their Cl^- or NO_3^- salts) in HEPES buffer solutions (50 mM, 30 mM NaCl, pH = 7.4, $CH_3CN–H_2O$ = 1 : 1, v/v). (b) The metal ion selectivity of probe L (498 nm). (Inset) The color change of L in a HEPES buffer solution (50 mM, 30 mM NaCl, pH = 7.4, $CH_3CN–H_2O$ = 1 : 1, v/v) without and with addition of $Zn(NO_3)_2$. (c) The fluorescence changes excited by a UV lamp (365 nm) and the color changes in probe L upon the addition of various metal cations. λ_{ex} = 363 nm. [L] = 0.1 mM, [M^{n+}] = 0.5 mM.

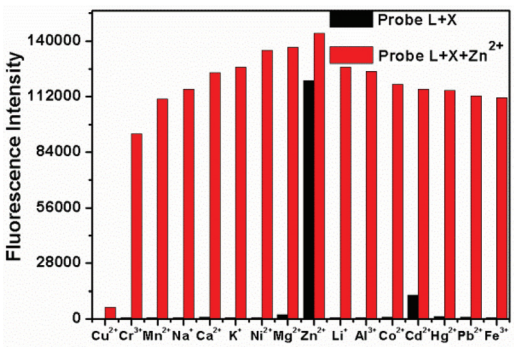

Fig. 5 The selectivity of L for Zn^{2+} in the presence of other metal ions in a HEPES buffer solution (50 mM, 30 mM NaCl, pH = 7.4, $CH_3CN–H_2O$ = 1 : 1, v/v). λ_{ex} = 363 nm. The black bars represent the addition of an excess of the appropriate metal ion (0.5 mM) to a 0.1 mM solution of L. The red bars represent the subsequent addition of 0.5 mM $Zn(NO_3)_2$ to the solution.

complex was hardly affected by other coexistent metal ions except Cu^{2+}, which often acts as a quencher *via* energy- or electron-transfer processes.[18] The quenching of the emission may be originated from the spin–orbit quenching mechanism associated with heavy metals, or the displacement of Zn^{2+} by Cu^{2+} from L–Zn^{2+}.[9a] Additionally, the absorption titration of L with Cu^{2+} was conducted in HEPES buffer (50 mM, 30 mM NaCl, pH = 7.40, $CH_3CN–H_2O$ = 1 : 1, v/v), and it was similar to that of L–Zn^{2+} (Fig. S3†). The stability constant of L–Cu^{2+} was 1.6×10^6 M^{-1} according to the nonlinear-fitting analysis of the absorption titration spectra (R^2 = 0.9988, Fig. S4†), which is a higher value than that of L–Zn^{2+}. The resulting plot confirms our hypothesis that Cu^{2+} could form complexes with L and then quench the fluorescence. However, Cu^{2+} would have the minimum interference with Zn^{2+} in living cells considering

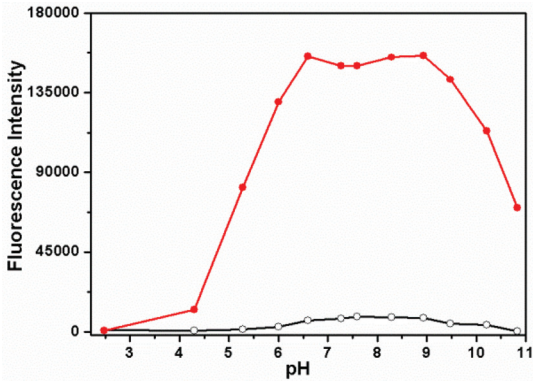

Fig. 6 The fluorescence intensities of L and L–Zn^{2+} at various pH values at room temperature in a HEPES buffer solution (50 mM, 30 mM NaCl, pH = 7.4, CH_3CN–H_2O = 1 : 1, v/v). λ_{ex} = 363 nm. Red line, the fluorescence intensities at 498 nm of L–Zn^{2+} at various pH values ([L] = 0.10 mM, [Zn^{2+}] = 0.1 mM); black line, the fluorescence intensities of L at various pH values ([L] = 0.10 mM).

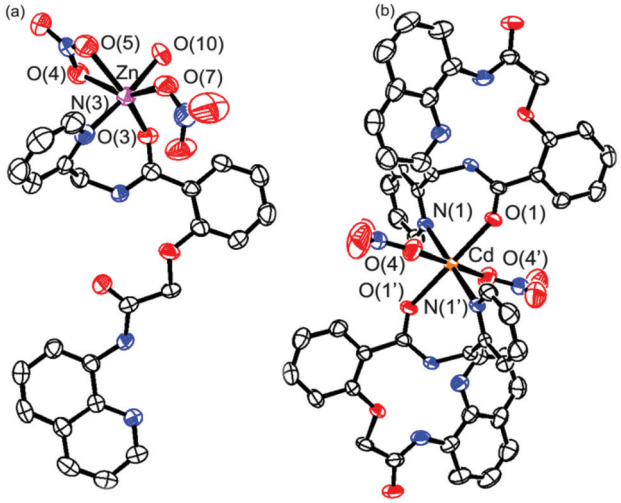

Fig. 7 The thermal ellipsoid (30% probability level) plot of (a) $ZnL(NO_3)_2(H_2O)$ and (b) $CdL_2(NO_3)_2$. All hydrogen atoms were deleted for clarity.

that it exists at a very low concentration only about 1/20 of Zn^{2+} in the human body.[9a,19,20]

The effect of pH

The pH dependency of the fluorescence of the system was determined by plotting the fluorescence intensity *vs.* the pH value in the presence and absence of Zn^{2+}, respectively (Fig. 6). The emission intensity of L–Zn^{2+} increased dramatically from pH ~ 2.5 to pH ~ 6.0, resulting from the competition between the proton and the zinc ion.[19,21] In particular, no significant change in the fluorescence spectra was observed in the range of pH 6–9 and it decreased under alkaline conditions. The quenching at a higher pH could be well explained by the formation of $Zn(OH)^-$ or $Zn(OH)_2$ and thus reducing the concentration of Zn^{2+}–L.[9a] The effect of pH on L–Cd^{2+} was also investigated as shown in Fig. S11.† It exhibited a stable fluorescence intensity at a pH range from 6 to 9 in the presence of Cd^{2+}, which is similar to that found in the L–Zn^{2+} system.

The crystal structure of $ZnL(NO_3)_2(H_2O)$ and $CdL_2(NO_3)_2$

The structures of the neutral complexes Zn^{2+} and Cd^{2+} were successfully characterized by X-ray crystallography as depicted in Fig. 7. They were synthesized from the same solvent but with different crystalline morphologies. The complex of Zn^{2+}, crystallizing in the monoclinic system and space group $P2_1/c$, consists of one crystallographically independent Zn^{2+} ion, one ligand L, one coordinated water molecule and two nitrates. Each Zn^{2+} is surrounded by one carbonyl oxygen atom and one pyridyl nitrogen atom coming from the ligand (N3, O3), three nitrate oxygen atoms (O4, O5, O7) and one oxygen atom (O10) from water. The Zn–O bond lengths vary from 1.978 (3) Å to 2.229(4) Å, and the bond length of Zn–N is 2.151(4) Å (Table S2†). However, the single-crystal X-ray analysis reveals that the complex CdL_2 $(NO_3)_2$ crystallizes in the triclinic system and space group $P\bar{1}$. The Cd^{2+} adopts an octahedral geometry and is six-coordinated by two carbonyl oxygen atoms and two pyridyl nitrogen atoms from two different ligands and two oxygen atoms from nitrate groups. The bond lengths of Cd–N and the two Cd–O are 2.316(2) Å, 2.348 (2) Å and 2.3026 (17) Å, respectively (Table S2†). As a general trend, the Cd^{2+}–N(O) distances is longer in comparison to the Zn^{2+} complex due to the larger ion radius of Cd^{2+}. The quinoline ring inclines parallel to the phenyl ring with the dihedral angle being 8.401° in the complex of Zn^{2+}, which is different from that in the Cd^{2+} complex which is 20.336°. In addition, the dihedral angle between the quinoline ring and the pyridyl ring in $ZnL(NO_3)_2(H_2O)$ (62.750°) is smaller than that in $CdL_2(NO_3)_2$ (80.365°). For sensor L, the chelating group would grasp Zn^{2+} in a suitable conformation, and the increased emission intensity of L might be ascribed to the "chelation enhancement of fluorescence" (CHEF). Meanwhile, the chelation of the ligand to Zn^{2+} effectively increases the coplanarity of the ligand and reduces the loss of energy *via* non-radiative transitions, leading to a larger fluorescence enhancement compared with Cd^{2+} and displaying the discriminating ability for Zn^{2+} over Cd^{2+}.

In the FTIR spectra, the characteristic amide carbonyl absorption at 1648 cm^{-1} of L was shifted to 1611 cm^{-1} for the Zn^{2+} compound and 1612 cm^{-1} for the Cd^{2+} compound, implying that a strong binding of the carbonyl group occurs with Zn^{2+} and Cd^{2+}. The presence of the quinoline skeleton was confirmed by the C=N stretching vibrations at ~1560 cm^{-1}.[22a] The vibration bands at 1480 cm^{-1}, 1280 cm^{-1}, 1030 cm^{-1} and 820 cm^{-1} of the complexes are attributed to NO_3^-. The significant changes at 400 cm^{-1}, 600 cm^{-1} and 1300 cm^{-1} suggest that the nitrogen atom coming from the pyridyl group is bonded to Zn^{2+} and Cd^{2+}.[22] The results that the metal ions were coordinated with the ligands are supported by the red-shift of the C=O stretching band, the changes of the characteristic absorption from the pyridyl group and the presence of an absorption peak assigned to NO_3^-.

Moreover, the ^{1}H NMR spectra of L–Cd^{2+}, L and L–Zn^{2+} were recorded. The proton signals for the b (CONH) and the a (CH_2) of the L–Zn^{2+} and L–Cd^{2+} systems all shift to a lower field relative to those of the ligand L (Fig. 8). However, for the b′ (CONH) and the a′ (CH_2), no apparent changes in the proton signals are seen after the addition of Zn^{2+} and Cd^{2+}. This indicates that the N atom in the pyridyl and O atom in the b (CONH) but the quinoline ring participates in the coordination environment of this system. Therefore, the coordination mode in solution is consistent with that in the solid state.

Computational studies

The hybrid density functional theory calculation was performed to make clear the electronic properties of this PET system. As we know, the analyte binding affects the energy position of either the HOMO or LUMO and the electronic distributions to a different degree, resulting in a significant change in the emission and absorption spectra.[23] The orbital energies of the system are presented in Fig. 9 for L, $CdL_2(NO_3)_2$, and its Zn^{2+} complex, $ZnL(NO_3)_2(H_2O)$, respectively.

As illustrated in Fig. 9, the π-electrons on the HOMO and LUMO of L are both mainly focused on quinoline. When Cd^{2+} is added, the energy level of both the LUMO and HOMO are higher than those of L. The slight increasing of the HOMO–LUMO gap indicates a shift in the absorption which correlates well with the experimental results. The distribution of the π-electrons on the HOMO and LUMO is similar to the L, locating at quinoline. This actually translates as little or no change in the emission character as the HOMO–LUMO gap is moderately affected.[24] However, in the presence of Zn^{2+}, it shows a significant change in the distribution of the π-electrons on the HOMO and LUMO. The energies of the HOMO and LUMO of the L–Zn^{2+} complex are much lower than those of L and L–Cd^{2+}. More importantly, the decreasing energy in the LUMO is more obvious than that of the HOMO. It suggests a smaller HOMO–LUMO gap and a bathochromic shift compared with L in absorption which may result from the increase of conjugation of the complex. These results strongly implied that the electron transfer process was greatly suppressed through the stabilization of the LUMO by the binding with Zn^{2+} and led to a larger fluorescence enhancement compared with Cd^{2+}.

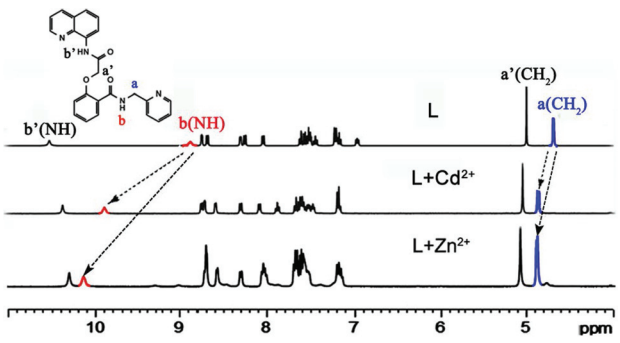

Fig. 8 The ^{1}H NMR spectra of L upon the addition of 2 equiv. of Zn^{2+} and Cd^{2+} in CD_3CN.

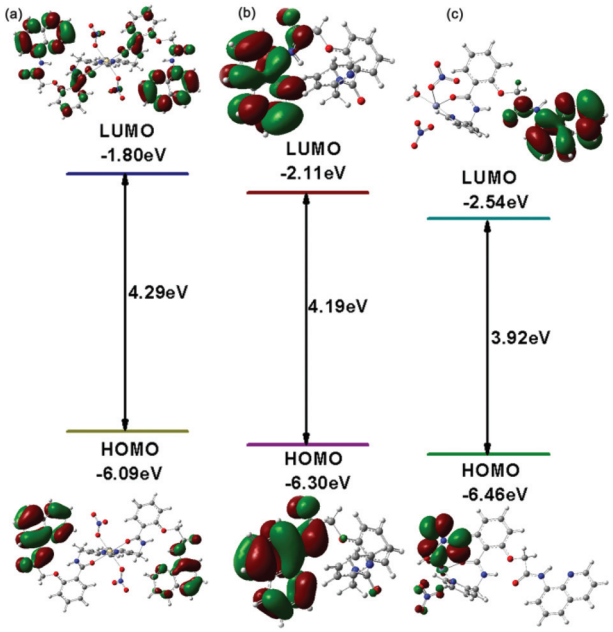

Fig. 9 The HOMO–LUMO energy gaps for the respective compounds and the interfacial plots of the orbitals: (a) L–Cd^{2+} complex; (b) L; (c) L–Zn^{2+} complex. The grey, red and blue atoms of the molecular frameworks indicate the C, O and N, respectively. The green and reddish brown parts on the interfacial plots refer to the different phases of the molecular wave functions, for which the isovalue is 0.02 au.

Fluorescence imaging of Zn^{2+} in living cells

Taking advantage of the excellent sensing properties for Zn^{2+} *in vitro*, the sensor was successfully used for the fluorescence imaging of Zn^{2+} in living cells. MCF-7 cells, one of the most representative and also the most common human cells in biological experiments, were used as targets to test Zn^{2+}. The incubation of the MCF-7 cells with 100 μM L alone in PBS buffer for 20 min at 37 °C gave a very weak intracellular fluorescence (Fig. 10c). However, when the cells were subsequently incubated with Zn^{2+} (300 μM) at 37 °C for another 30 min, a green fluorescence was displayed (Fig. 10d). The results of the bright-field measurements (Fig. 10a and 10b) suggested that the cells were viable throughout the imaging experiments upon treatment with L and Zn^{2+}, respectively. As depicted, the obvious changes confirm the fluorescence enhancement with excellent cell permeability. These results suggested that L is biocompatible in nature and could be used for detecting Zn^{2+} in living cells rapidly.

Conclusions

In summary, an off–on fluorescent sensor that can give different fluorescence responses to Zn^{2+} and Cd^{2+} was studied, the sensing and binding properties of L were fully exploited.

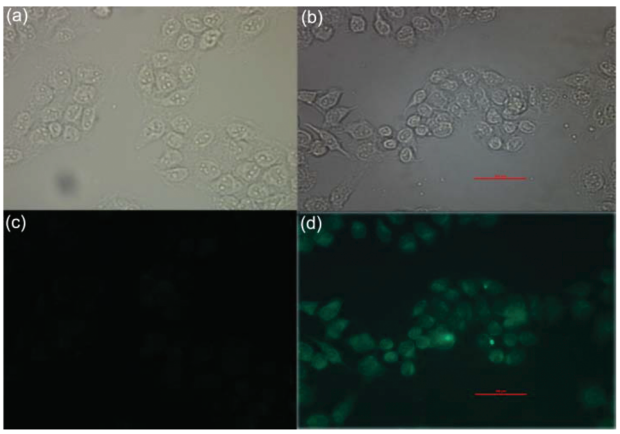

Fig. 10 Bright-field transmission images of MCF-7 cells incubated with (a) 100 μM L for 20 min, (b) and then further incubated with 300 μM $Zn(NO_3)_2$ for 30 min. (c), (d) Fluorescence images of MCF-7 cells in (a) and (b). Scale bar: 100 μm.

The X-ray crystal structure analysis reveals that sensor L coordinates to Zn^{2+} *via* a 1 : 1 binding mode but to Cd^{2+} *via* a 2 : 1 binding mode, which leads to the different spatial arrangement of the fluorogenic unit in these complexes. Additionally, the recognition mechanisms of L toward Zn^{2+} and Cd^{2+} were further attempted to explain by computational results. The results establish that the chemosensor can serve as a highly sensitive probe for distinguishing Zn^{2+} from Cd^{2+} by a different binding mode, molecular orbital energy levels and electron transitions. The utility of L was demonstrated in cell bioimaging.

Acknowledgements

The authors acknowledge financial support from the NSFC (grants 20931003 and 91122007) and the Specialized Research Fund for the Doctoral Program of Higher Education (grant 20110211130002).

References

1 (*a*) R. Y. Tsien, in *Fluorescent and Photochemical Probes of Dynamic Biochemical Signals inside Living Cells*, ed. A. W. Czarnik, American Chemical Society, Washington, DC, 1993; (*b*) G. Hennrich, H. Sonnenschein and U. Resch-Genger, *J. Am. Chem. Soc.*, 1999, **121**, 5073; (*c*) Y. H. Lee, M. H. Lee, J. F. Zhang and J. S. Kim, *J. Org. Chem.*, 2010, **75**, 7159; (*d*) A. Mokhir, A. Kiel, D. Herten and R. Kraemer, *Inorg. Chem.*, 2005, **44**, 5661.

2 (*a*) F. A. Cotton and G. Wilkinson, *Advanced Inorganic Chemistry*, Wiley, 5th edn, 1988; (*b*) J. M. Berg and Y. Shi, *Science*, 1996, **271**, 1081; (*c*) C. J. Frederickson, J.-Y. Koh and A. I. Bush, *Nat. Rev. Neurosci.*, 2005, **6**, 449.

3 (*a*) S. J. Lippard and J. M. Berg, *Principles of Bioinorganic Chemistry*, University Science Books, Mill Valley, CA, 1st edn, 1994; (*b*) B. L. Vallee and K. H. Falchuk, *Psychol. Rep.*, 1993, **73**, 79; (*c*) S. L. Sensi, L. M. Canzoniero, S. P. Yu, H. S. Ying, J. Y. Koh, G. A. Kershner and D. W. Choi, *J. Neurosci.*, 1997, **17**, 9554; (*d*) J. E. Coleman, *Curr. Opin. Chem. Biol.*, 1998, **2**, 222.

4 (*a*) A. I. Bush, W. H. Pettingell, G. Multhaup, M. Paradis, J.-P. Vonsattel, J. F. Gusella, K. Beyreuther, C. L. Masters and R. E. Tanzi, *Science*, 1994, **265**, 1464; (*b*) J. H. Weiss, S. L. Sensi and J. K. Koh, *Trends Pharmacol. Sci.*, 2000, **21**, 395; (*c*) S. W. Suh, K. B. Jensen, M. S. Jensen, D. S. Silva, P. J. Kesslak, G. Danscher and C. J. Frederickson, *Brain Res.*, 2000, **852**, 274; (*d*) A. I. Bush, *Alzheimer Dis. Assoc. Disord.*, 2003, **17**, 147; (*e*) X. Q. Chen, T. H. Pradhan, F. Wang, J. S. Kim and J. Y. Yoon, *Chem. Rev.*, 2012, **112**, 1910.

5 E. L. Que, D. W. Domaille and C. J. Chang, *Chem. Rev.*, 2008, **108**, 1517.

6 (*a*) N. C. Lim, H. C. Freake and C. Brückner, *Chem.–Eur. J.*, 2005, **11**, 38–49; (*b*) Z. C. Xu, J. Y. Yoon and D. R. Spring, *Chem. Soc. Rev.*, 2010, **39**, 1996–2006; (*c*) H. G. Lee, J. H. Lee, S. P. Jang, H. M. Park, S. Kim, Y. Kim, C. Kim and R. G. Harrison, *Tetrahedron*, 2011, **67**, 8073–8078; (*d*) E. Kimura and T. Koike, *Chem. Soc. Rev.*, 1998, **27**, 179.

7 (*a*) P. G. Jiang and Z. Guo, *Coord. Chem. Rev.*, 2004, **248**, 205–229; (*b*) X. Tang, X. Peng, W. Dou, J. Mao, J. Zheng, W. Qin, W. Liu, J. Chang and X. Yao, *Org. Lett.*, 2008, **10**, 3653–3656; (*c*) E. M. Nolan, J. W. Ryu, J. Jaworski, R. P. Feazell, M. Sheng and S. J. Lippard, *J. Am. Chem. Soc.*, 2006, **128**, 15517; (*d*) K. Komatsu, K. Kikuchi, H. Kojima, Y. Urano and T. Nagano, *J. Am. Chem. Soc.*, 2005, **127**, 10197; (*e*) N. C. Lim, J. V. Schuster, M. C. Porto, M. A. Tanudra, L. Yao, H. C. Freake and C. Brückner, *Inorg. Chem.*, 2005, **44**, 2018–2030; (*f*) M. M. Henary, Y. G. Wu and C. J. Fahrni, *Chem.–Eur. J.*, 2004, **10**, 3015; (*g*) S. Y. Jiao, L. L. Peng, K. Li, Y. M. Xie, M. Z. Ao, X. Wang and X. Q. Yu, *Analyst*, 2013, **138**, 5762; (*h*) G. Sivaraman, T. Anand and D. Chellappa, *Analyst*, 2012, **137**, 5881.

8 (*a*) G. Svehla and G. Suehla, *Vogel's Qualitative Inorganic Analysis*, Addison-Wesley, 7th edn, 1996; (*b*) K. Soroka, R. S. Vithanga, D. A. Philips, B. Walker and P. K. Dasgupta, *Anal. Chem.*, 1987, **59**, 629; (*c*) L. Xue, H. H. Wang, X. J. Wang and H. Jiang, *Inorg. Chem.*, 2008, **47**, 4310–4318; (*d*) J. L. Wang, W. Y. Lin and W. L. Li, *Chem.–Eur. J.*, 2012, **18**, 13629–13632.

9 (*a*) X. Y. Zhou, B. R. Yu, Y. L. Guo, X. L. Tang, H. H. Zhang and W. S. Liu, *Inorg. Chem.*, 2010, **49**, 4002; (*b*) X. Y. Zhou, P. X. Li, Z. H. Shi, X. L. Tang, C. Y. Chen and W. S. Liu, *Inorg. Chem.*, 2012, **51**, 9226–9231; (*c*) J. Jiang, H. Jiang, X. Tang, L. Yang, W. Dou, W. Liu, R. Fang and W. Liu, *Dalton Trans.*, 2011, **40**, 6367.

10 Y. Mikata, Y. Sato, S. Takeuchi, Y. Kuroda, H. Konno and S. Iwatsuki, *Dalton Trans.*, 2013, **42**, 9688.

11 (*a*) Z. Jiri, P. Magdalena, H. Petr and T. Milos, *Synthesis*, 1994, 1132; (*b*) X. Y. Zhou, Y. L. Guo, Z. H. Shi, X. Q. Song, X. L. Tang, X. Hu, Z. T. Zhu, P. X. Li and W. S. Liu, *Dalton Trans.*, 2012, **41**, 1765.

12 (*a*) *SMART, 5.05 ed*, Bruker AXS, Inc., Madison, WI, 1998; (*b*) *SAINT, version 6.45*, Bruker AXS, Inc., Madison, WI, 1997.
13 G. M. Sheldrick, *SADABS: Area-Detector Absorption Correction*, University of Göttingen, Göttingen, Germany, 1996.
14 G. M. Heldrick, *SHELXL-97, Program for the Refinement of Crystal Structures*, University of Göttingen, Göttingen, Germany, 1997.
15 M. J. Frisch, *Gaussian 09, revision A.01*, Gaussian, Inc., Wallingford, CT, U.S.A., 2009.
16 (*a*) A. D. Becke, *J. Chem. Phys.*, 1993, **98**, 5648–5652; (*b*) C. Lee, W. Yang and R. G. Parr, *Phys. Rev. B*, 1988, **37**, 785–789; (*c*) P. J. Hay and W. R. Wadt, *J. Chem. Phys.*, 1985, **82**, 270; (*d*) W. R. Wadt and P. J. Hay, *J. Chem. Phys.*, 1985, **82**, 284; (*e*) P. J. Hay and W. R. Wadt, *J. Chem. Phys.*, 1985, **82**, 299.
17 J. A. Zhou, X. L. Tang, J. Cheng, Z. H. Ju, L. Z. Yang, W. S. Liu, C. Y. Chen and D. C. Bai, *Dalton Trans.*, 2012, **41**, 10626.
18 Y. M. Yang, Q. Zhao, W. Feng and F. Y. Li, *Chem. Rev.*, 2013, **113**, 192–270.
19 L. Xue, G. P. Li, D. J. Zhu, Q. Liu and H. Jiang, *Inorg. Chem.*, 2012, **51**, 10842–10849.
20 (*a*) J. Luo, W. S. Li, P. Xu, L. Y. Zhang and Z. N. Chen, *Inorg. Chem.*, 2012, **51**, 9508–9516; (*b*) K. Komatsu, Y. Urano, H. Kojima and T. Nagano, *J. Am. Chem. Soc.*, 2007, **129**, 13447–13454.
21 Y. Zhang, X. F. Guo, W. X. Si, L. H. Jia and X. H. Qian, *Org. Lett.*, 2008, **10**, 473–476.
22 (*a*) H. P. Wang, Y. F. Ma, H. Tian, N. Tang, W. S. Liu, Q. Wang and Y. Tang, *Dalton Trans.*, 2010, **39**, 7485–7492; (*b*) A. K. Talal, A. Al-Ailaf and Z. M. Shfft, *Polyhedron*, 1995, **14**, 239–248; (*c*) W. H. Robert and C. Thoms, *Polyhedron*, 1998, **17**, 4347–4352.
23 (*a*) Y. P. Li, H. R. Yang, Q. Zhao, W. C. Song, J. Han and X. H. Bu, *Inorg. Chem.*, 2012, **51**, 9642–9648; (*b*) J. Mcgrier, P. L. Bunz and U. H. F. Bunz, *Acc. Chem. Res.*, 2010, **43**, 397.
24 O. B. Bozdemir, R. Guliyev, O. Buyukcakir, S. Selcuk, S. Kolemen, G. Gulcihan, T. Nalbantoglu, H. Boyaci and E. U. Akkaya, *J. Am. Chem. Soc.*, 2010, **132**, 8029.